Structural Noise In Modelisation

Bertrand CHASSIGNOLE, EDF, Paris, France, Julien DIAZ, INRIA France,
Veronique DUWIG Thierry FOUQUET and Andreas SCHUMM, EDF, Paris, France

Abstract. In this paper we present two methods to modelize structural noise. The first one simulates the propagation in the grains of a material, the second one respresents the attenuation with a new model.

1 Introduction

One of the remaining problems in ultrasonic modelling is to take into account structural noise due to scattering effects within the granular microstructure of polycrystalline metal welds. The term "structural noise" refers to two effects usually observed: The scattering effects due to propagation across grains with different orientation and sound velocity create secondary waves, which can be observed as noise, and attenuate the energy of the primary incident wave. Both effects reduce the signal to noise ratio of the received echo, and are therefore vital to be taken into account in quantitative modelling.

In this paper, we consider two approaches to implement structural noise or only attenuation in our modelling code ATHENA, based on a finite element method on a regular mesh with a fictitious domain method for arbitrarily shaped defects [5].

In a finite element model, it is particularly tempting to work directly at a grain scale, representing the granular structure by the mesh. Since the grains of polycrystalline metals are typically larger than the mesh elements in our finite element model, this approach does not introduce further mesh refinements, which would be prohibitive in terms of computation cost. To represent the granular structure, we assume that the different grains share the same elastodynamic properties, and differ only in terms of a rotation angle. In order to apply this model, which should be strictly valid only in three dimensions, we further assume that the grain rotation takes place around an axis belonging to the symmetry plane [3].

A second, simpler approach consists in modeling only the attenuation effect, by adding a damping term in the equations we have to solve, resulting in an energy decay. We consider a model for which we can construct an explicit stable discretisation. It allows us to introduce anisotropic attenuation without sacrificing the advantageous properties of our code

2 The elastic model implemented in Athena

In this chapter we briefly describe the model implemented in Athena, while insisting on the properties we want to conserve in our future method. In the following we consider a cracked solid in two dimension, but the method has been extended to three dimensions. Let us call Ω the open domain occupied by the solid and $\partial\Omega$ its boundary. We also denote Γ the crack. τ is the tangential vector and n the normal one. As we will work with the strainth-velocity formulation, we denote σ the strength tensor and $v = (v_x, v_y)$, the displacement velocity and $\epsilon(v) = \frac{1}{2}(\nabla v + \nabla^T v)$, ρ the density.

2.1 The continuous problem

The Hook law written in strenth velocity terms is

$$\frac{\partial \sigma}{\partial t} = C\varepsilon(v) \quad \text{in } \Omega\,. \tag{1}$$

The elasticity tensor C is a 4×4 symmetric, positive tensor, we denote A its inverse. The law of conservation gives

$$\rho \frac{\partial v}{\partial t} - div\,\sigma = f \quad \text{in } \Omega\,, \tag{2}$$

where f can be a source. The crack is modelied by a free surface condition $\sigma.n_\Omega = 0 \quad \text{sur } \partial\Omega\,.$

To obtain a discretisation of the equation by a finite element method we need to construct the variational formulation and thus to introduce some functional space where we will look for the solutions.

$$\begin{aligned} V &= (L^2(\Omega))^2, \\ H &= \{\sigma \in H_{div}(\Omega),\ \sigma \text{ symetric and } \sigma.n = 0 \text{ on} \partial\Omega\}\ . \end{aligned}$$

The variationnal formulation writes:

$$\text{find } w \in V, \sigma \in H \text{ and } \in L \text{ such that} \tag{3}$$

$$\frac{d}{dt}\int_\Omega A\sigma : \Sigma + \int_\Omega v.div\Sigma - \int_\Gamma (\Sigma.n).\lambda = 0\,, \forall \Sigma \in H \tag{4}$$

$$\frac{d}{dt}\int_\Omega \rho v.w - \int_\Omega div\sigma.w = \int_\Omega f.w\,, \forall v \in V \tag{5}$$

$$\int_\Gamma (\sigma.n).\mu = 0\,, \forall \mu \in L\,. \tag{6}$$

where $\lambda = [w] = w^+ - w^-$, a Lagrange multiplyer, is the velocity jump on the crack and $L = H_{00}^{\frac{1}{2}}(\Gamma)$.

2.2 The numerical scheme.

We can now discretise the previous formulation with finite element. We choose the $Q_1 - Q_0$ elements, which allow us to use mass lumping in order to obtain an quasi-explicit scheme (the mass matrix M_σ is diagonal by 5×5 block and M_v is diagonal) [5]

$$M_\sigma \frac{\sigma^{n+\frac{1}{2}} - \sigma^{n-\frac{1}{2}}}{\Delta t} + K\,V^n - B^T\Lambda^n = 0 \tag{7}$$

$$M_v \frac{V^{n+1} - V^n}{\Delta t} - K^T\sigma^{n+\frac{1}{2}} = F^{n+\frac{1}{2}} \tag{8}$$

$$B\sigma^{n+\frac{1}{2}} = 0\,, \tag{9}$$

where $F^{n+\frac{1}{2}}$ is a discretisation in space of f at the time step $n + \frac{1}{2}$.

Multiplying (7) by BM_σ^{-1} and using (9) one can obtain the relation to compute Λ.

$$\Lambda^n = (BM_\sigma^{-1}B^T)^{-1}BM_\sigma^{-1}KV^n\,. \tag{10}$$

One can notice that the dimension of the matrix $BM_\sigma^{-1}B^T$ equals the number of points on the crack, and is thus not too expensive to inverse.

The scheme is thus quasi explicit and can take into account cracks of complex geometry even if the volume mesh is structured, thanks to the fictitious domain method. One can show that this scheme is stable under the C.F.L. condition

$$c_P\frac{\Delta t}{\Delta x} \leq 1\ ,$$

where c_P is the velocity of P waves.

3 Modelisation of the structural noise at the grain scale.

In this part we present a way to take into account the grains of the material during elastodynamic wave propagations. Let us assume that the grains only differ from the anisotropic axis of the material. It is thus necessary to be able to describe a three dimensional orientation of a material, but we would like to stay with the two dimensional equation, to keep a rapid calculation. Furthermore, as we can not have the precise descriptions of each grain we will construct our domain with some random media.

3.1 Presentation of the model

Here we are only going to present the modifications brought to the "classical" 2D model. One can consult [5] for more details about this method. Classically the 2D model is obtained from the 3D model assuming two hypothesis : Firstly, the problem is invariable with a translation in a direction and secondly that one of the orthotropic axis coincides with that direction. The system can then be split in two independant system. For example if that direction is the axis Oz, one obtains

$$\begin{cases} \dfrac{\partial}{\partial t}\begin{bmatrix}\sigma_{xx}\\ \sigma_{yy}\\ \sigma_{xy}\end{bmatrix} = \begin{bmatrix} c_{11} & c_{12} & c_{16}\\ c_{12} & c_{22} & c_{26}\\ c_{16} & c_{26} & c_{66}\end{bmatrix}\begin{bmatrix} \dfrac{\partial u}{\partial x}\\ \dfrac{\partial v}{\partial y}\\ \dfrac{1}{2}\left(\dfrac{\partial u}{\partial y}+\dfrac{\partial v}{\partial x}\right)\end{bmatrix} & \text{(11a)}\\[2ex] \rho\dfrac{\partial}{\partial t}\begin{bmatrix}u\\ v\end{bmatrix} = \begin{bmatrix}\dfrac{\partial \sigma_{xx}}{\partial x}+\dfrac{\partial \sigma_{xy}}{\partial y}\\ \dfrac{\partial \sigma_{xy}}{\partial x}+\dfrac{\partial \sigma_{yy}}{\partial y}\end{bmatrix} & \text{(11b)} \end{cases}$$

and

$$\begin{cases} \dfrac{\partial}{\partial t}\begin{bmatrix} \sigma_{yz} \\ \sigma_{xz} \end{bmatrix} = \begin{bmatrix} c_{44}\ c_{45} \\ c_{45}\ c_{55} \end{bmatrix} \begin{bmatrix} \dfrac{1}{2}\dfrac{\partial w}{\partial y} \\ \dfrac{1}{2}\dfrac{\partial w}{\partial x} \end{bmatrix} & \text{(12a)} \\ \rho\dfrac{\partial w}{\partial t} = \dfrac{\partial \sigma_{xz}}{\partial x} + \dfrac{\partial \sigma_{yz}}{\partial y} & \text{(12b)} \end{cases}$$

System (11) represents the classical elastodynamic equations in two dimensions. In our case, we are not going to consider the hypothesis on the anisotropy of the material anymore, but only the fact that the problem is invariable in one direction. This makes disappear σ_{zz} but we are lead to solve a system with three more unknown (σ_{xz}, σ_{yz} and w)

$$\begin{cases} \dfrac{\partial}{\partial t}\begin{bmatrix} \sigma_{xx} \\ \sigma_{yy} \\ \sigma_{yz} \\ \sigma_{xz} \\ \sigma_{xy} \end{bmatrix} = \begin{bmatrix} c_{11}\ c_{12}\ c_{14}\ c_{15}\ c_{16} \\ c_{12}\ c_{22}\ c_{24}\ c_{25}\ c_{26} \\ c_{14}\ c_{24}\ c_{44}\ c_{45}\ c_{46} \\ c_{15}\ c_{25}\ c_{45}\ c_{55}\ c_{56} \\ c_{16}\ c_{26}\ c_{46}\ c_{56}\ c_{66} \end{bmatrix} \begin{bmatrix} \dfrac{\partial u}{\partial x} \\ \dfrac{\partial v}{\partial y} \\ \dfrac{1}{2}\left(\dfrac{\partial w}{\partial y}\right) \\ \dfrac{1}{2}\left(\dfrac{\partial w}{\partial x}\right) \\ \dfrac{1}{2}\left(\dfrac{\partial u}{\partial y} + \dfrac{\partial v}{\partial x}\right) \end{bmatrix} & \text{(13a)} \\ \rho\dfrac{\partial}{\partial t}\begin{bmatrix} u \\ v \\ w \end{bmatrix} = \begin{bmatrix} \dfrac{\partial \sigma_{xx}}{\partial x} + \dfrac{\partial \sigma_{xy}}{\partial y} \\ \dfrac{\partial \sigma_{xy}}{\partial x} + \dfrac{\partial \sigma_{yy}}{\partial y} \\ \dfrac{\partial \sigma_{xz}}{\partial x} + \dfrac{\partial \sigma_{yz}}{\partial y} \end{bmatrix} & \text{(13b)} \end{cases}$$

We can underline that if there are more unknown the system is not as expensive to solve as the 3D problem, as the domain is still in two dimension. The variational formulation is formally the same as (7), but behind the equations there are three more unknowns.

3.2 The numerical scheme

One can show that the variational formulation leads to search w in the same approximation space than u and v, and σ_{xz} (resp. σ_{yz}) in the same space approximation than σ_{xx} (resp. σ_{yy}). The formulation is then

$$\begin{cases} \dfrac{\mathrm{d}}{\mathrm{d}t} M_\sigma \Sigma + B^T V = 0 & \text{(14a)} \\ \dfrac{\mathrm{d}}{\mathrm{d}t} M_v V - B\Sigma = 0. & \text{(14b)} \end{cases}$$

where

$$\Sigma = \left[\sigma_{xx}^h,\, \sigma_{xx}^b,\, \sigma_{yy}^d,\, \sigma_{yy}^g,\, \sigma_{xy},\, \sigma_{xz}^h,\, \sigma_{xz}^b,\, \sigma_{yz}^d,\, \sigma_{yz}^g\right]^t.$$

and

$$V = [u,\, v,\, w]\,.$$

Here, the Matrix M_σ is a diagonal by 9×9 block where it is 5×5 block in the classical model and 18×18 block in the full 3D problem. Compared to the 2D formulation, we have on each node one more velocity unknown and four more strenth unknowns (two for each σ_{xz} and σ_{yz}). So there are twelve unknowns instead of seven, but there are still less unknowns than in the 3D version (21). We can also mention that as we are still in a 2D case, the domain is represented by a 2D mesh. Furthermore it is easy to validate the code obtained with some reference calculus made with the 3D code for an 3D anisotropic material.

Remark 1 *The addition of those unknowns does not affect the stability of the method. The modification needed for the PML equations can be done in the same way, and the modification needed to the fictitious domain method only leads to add a new unknown on the vector* Λ *(*λ_z*)*

3.3 Construction of a random medium

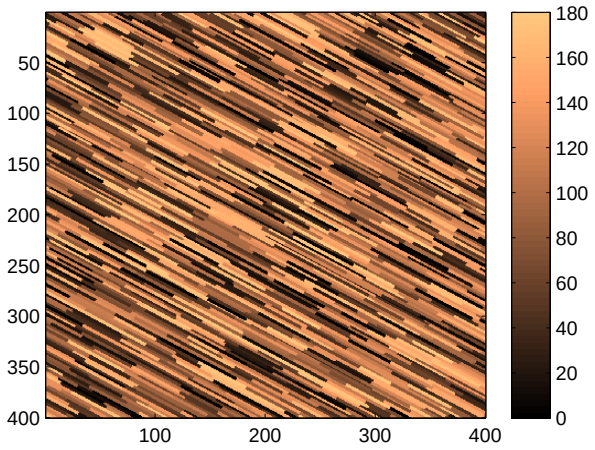

Figure 1: an example of a random medium

To be able to simulate wave propagation in a complex medium like a weld, we have to consider the construction of random heterogeneous media. We will first present the construction of a medium where all the grains are oriented in the same direction and then we will show how to extend the construction to more complex situations.

We have considered some gaussian laws for the size of the grains, but this choice is in fact not very important in the construction. Let us consider the case with all the grains oriented parallel to the axis Oy. We split the interval [0 x] in n_i intervals following the probability law of the width of the grain. For each column obtained we divide in n_j intervals according to the probability law of the length of the grains. Then we affect randomly an angle of rotation to each grain.

If the grain axis [100] is oriented at an angle *theta* with the axis Ox, we do the same construction but on a rectangle large enough so that when we carry out the rotation the entire domain is still covered. An exemple of such a medium is given in Figure 1 (the color scale represents the angles of rotation around the axis [100]). It might not be clear on the figure but such a construction leads to a step wedge mesh for the grains because of the structured character of the mesh.

In the case of the weld, we consider that the weld is composed of areas in which all the grains have the same orientation in the incidence plane, but can be rotated in the plane perpendicular to the incidence plane. Then to construct our media, for each region, we make the previous construction for a rectangle larger than the area, keeping only the part of the interesting region. An example of a weld is given Figure 2

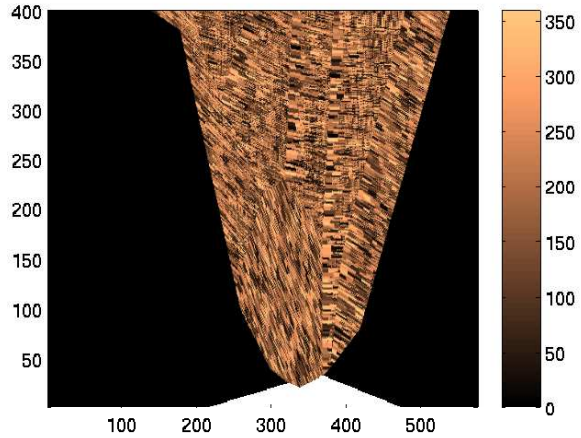

Figure 2: An example of a weld, the black part is an isotropic area

3.4 Numerical experiment

In this section we are interested in the simulation of wave propagation in a piece of metal of dimension $40mm \times 40mm$ with all the grains with the same orientation i.e. 45 degree to the vertical axis. The source is situated on the top of the metal and has a length of 6.5mm. The waves generated are P-waves. The frequency of the source is 2MHz. We present on Figures 3 to 8 snapshots of the velocity modulus for t =1.6, 3.2, 4.8, 6.4, 8 and 9.6 µs. Those snapshots show clearly the structural noise.

To have a more precise idea of the phenomena, we present on Figure 9 the variation of the normal component of the velocity recorded by the transducer. We can clearly distinguish two parts.

- The coherent signal, attenuated compared to the one we would have obtained with an homogeneous material.
- The noise induced by the multiple reflections of the wave on the grain.

To emphasize the phenomena we present on Figure 10 the previous signal (in red) and the signal obtained with an homogeneous material with the characteristic of a single grain (in blue). The noisy signal is significantly attenuated and the travel times are

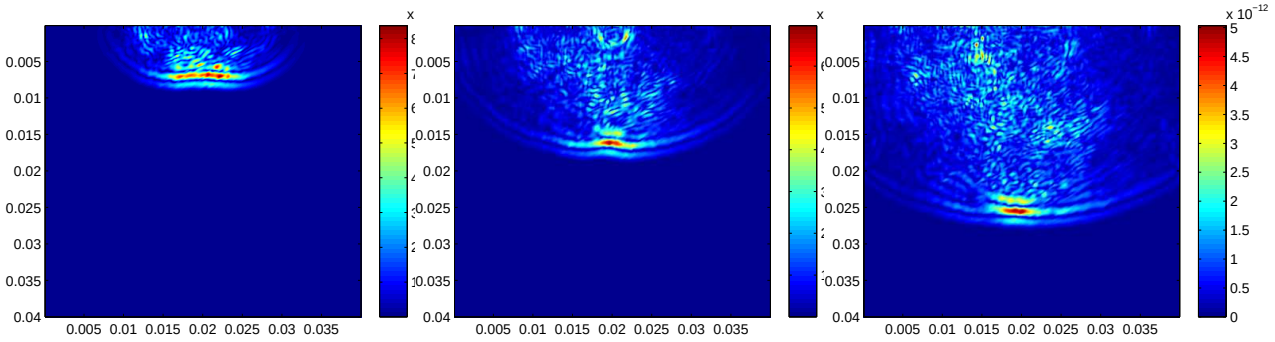

Figure 3: t=1.6 µs Figure 4: t=3.2 µs Figure 5: t=4.8 µs

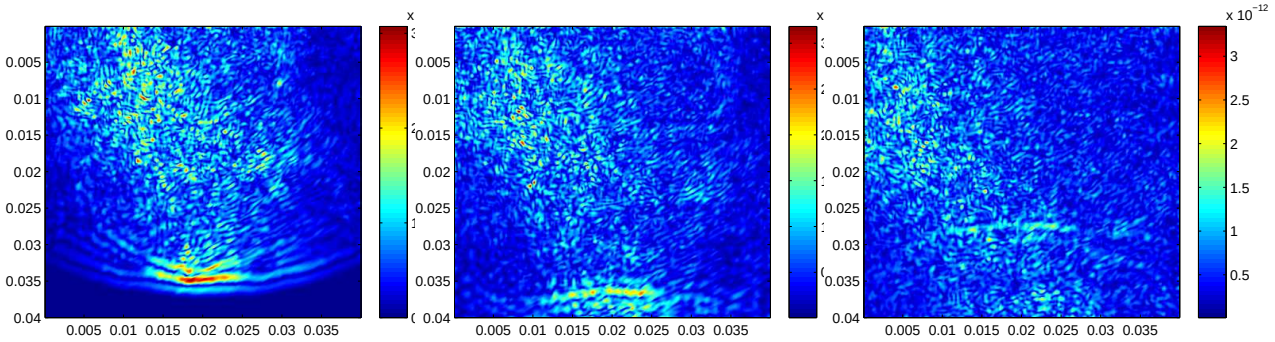

Figure 6: t=6.4 µs Figure 7: t=8 µs Figure 8: t=9.6 µs

slightly different. This is due to the fact that the structure of the grains modifies the propagation speeds.

To identify some average effect, we do the same experiment on a set of 100 random materials but still with an orientation of 45 degrees. On Figure 11 we compare the previous signal with the average signal. The noise has almost disappeared.

We now want to compare the attenuation obtained with what we should have obtained. Results from previous theoretical work [1] show that the attenuation of the coherent signal (i.e. the first part of the signal), raises when the orientation of the grains varies from 0° to 90°. We tried to verify this property by studying the effect on grains orientation. Let us denote

- S_{ref} the Fourier transform of the reference signal (blue one on Figure 10) ;
- S the Fourier transform of the coherent signal ;
- $a = 20log(S/S_ref)/L$ the attenuation (in dB/mm) where L is the length of the material.

We make the previous experiment for different orientations : $0, 15, 30, 45, 60, 75$ and $90°$. For each orientation we generate 100 different media and make the previous numerical experiment and we present on Figure 12 the attenuation obtained with the frequency for differents angles. The curves are not clearly separated but we can see that for frequencies between 2MHz and 2.5Mhz, which are the frequencies considered in [1] the attenuation increases with the angle until 45° and then decays. This shows a contradiction with the theory. A possible explanation can come from the step wedge

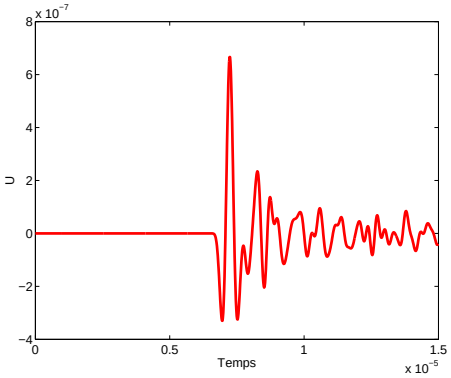

Figure 9: signal obtained on the transducer.

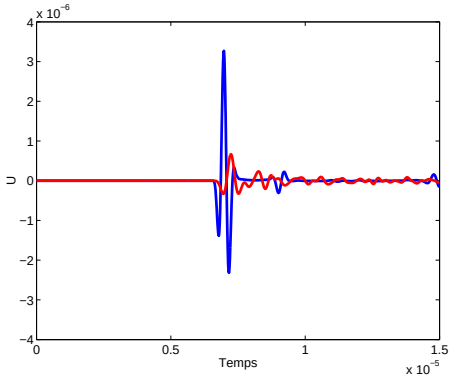

Figure 10: signal obtained on the transducer (red) and signal obtained for an homogeneous media (blue).

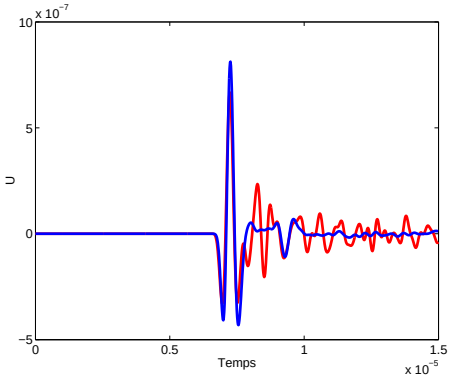

Figure 11: Signal for one experiment (in red) and the average on 100 signals (in blue).

mesh. At 45° our mesh is the farest from reality, but since we used a very fine mesh this hypothesis seems weak. Some new experiments should answer this question. By rotating the source instead of rotating the mesh we should know if it is an effect of the mesh. Other explanations are possible. We are not sure that the choice we made to describe the grains is realistic - the gaussian law describing the grain size might be inappropriate. We chose a fully random distribution for the angle of rotation around the axe [100], but it might be that some coherence exists due to the fabrication of weld. In any case, once validated, this model can be useful because it allows to vary parameters easily and it also provides an easy way to make experiments with T-waves at 0°, which is difficult to do in real experiments. We think that the model could provide numerous results on the attenuation for example for a macroscopic model.

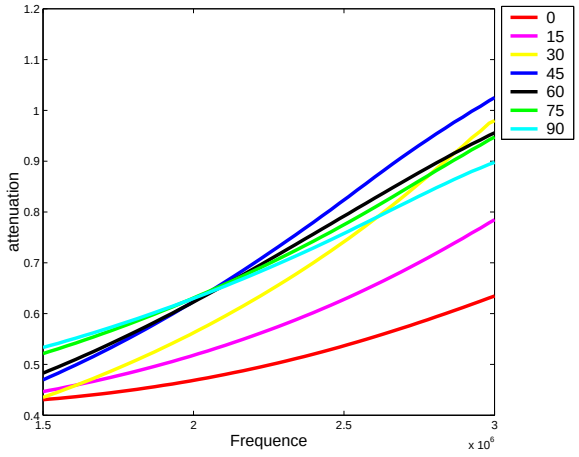

Figure 12: Attenuation as a function of frequency for different orientation.

4 Modeling of attenuation

We propose to integrate a model of anisotropic heterogeneous attenuation in the code Athena. We want to keep the same advantages as in the elastodynamic version that are:

- the possibility of modeling the cracks with the fictitious domains;
- the modeling of unbounded domains thanks to the Perfectly Matched Layers (PML);
- a low cost simulation because of the resolution of a quasi-explicit scheme after discretization by finite elements in space and finite differences in time.

If possible, we would prefer to avoit to add further variables or equations.

4.1 A "time attenuation"

Let us assume that we are in dimension 1 and consider a plane wave with a pulsation ω and a wave number k:

$$v = v^0 \exp(i(\omega t - kx)) .$$

This is the solution of the wave equation. The wave number k is real and equal to $k = \pm\frac{\omega}{c}$. There is no attenuation because the wave amplitude remains equal to $|v^0|$. For a positive wave number ($k > 0$), the propagation is in the sense of the raising x and for a negative wave number ($k < 0$), the propagation is in the sense of the decreasing x.

We are trying to modify the elastodynamic equations in order to obtain a solution like an "attenuated plane wave"

$$v = v^0 \exp(-\gamma x) \exp(i(\omega t - k_1 x)) \,,$$

where the space attenuation number γ has the same sign as k_1, that is positive for a wave propagating in the sense of the raising x and negative for a wave propagating in the sense of the decreasing x.

Given that the time evolves only in one direction, it is easier to add a time attenuation than a space attenuation in the equation. The "time attenuated plane wave" can be written as

$$v = v^0 \exp(-(\gamma c)t) \exp(i(\omega t - k_1 x)) \,,$$

where the time attenuation number γc is positive for all k_1.

4.2 The equations

The attenuation model's equations are the following

$$\begin{aligned} \frac{\partial \sigma}{\partial t} + D\sigma &= C\varepsilon(v) \quad \text{in } \Omega \,, \\ \rho \frac{\partial v}{\partial t} - div\, \sigma &= f \quad \text{in } \Omega \\ \sigma.n &= 0 \quad \text{on } \Gamma \,. \end{aligned}$$

The attenuation comes from the tensor D. For $D = 0$ we have the elastodynamic equations. We have proven that this attenuated problem is well posed (existence and uniqueness of the solution) when the tensor C is symmetrical and positive definied and when the tensor $C^{-1}D$ is symmetrical and positive. Note that this attenuated model does not represent exactly the physical phenomena. The tensor C no longer represents the elastic tensor and the values of both tensors C and D have no physical signification.

4.3 The numerical scheme

We use the same space discretization as in the elastodynamic case. We introduce a "stress attenuation matrix" M_D built like the stress mass matrix M_σ but with the tensor $C^{-1}D$ instead of the tensor C^{-1}. Then we define two "modified mass matrices" M_σ^+ et M_σ^-,

$$M_\sigma^+ = M_\sigma + \frac{\Delta t}{2} M_D \quad \text{et} \quad M_\sigma^- = M_\sigma - \frac{\Delta t}{2} M_D \,.$$

The new scheme is

$$\begin{aligned} \frac{M_\sigma^+ \sigma^{n+\frac{1}{2}} - M_\sigma^- \sigma^{n-\frac{1}{2}}}{\Delta t} + K\, V^n - B^T \Lambda^n &= 0 \\ M_v \frac{V^{n+1} - V^n}{\Delta t} - K^T \sigma^{n+\frac{1}{2}} &= F^{n+\frac{1}{2}} \\ B\sigma^{n+\frac{1}{2}} &= 0\,. \end{aligned}$$

The only difference for the attenuated scheme compared to the elastodynamic scheme is the presence of two modified mass matrices M_σ^+ et M_σ^- instead of one mass matrix M_σ. Note that M_σ^+ and M_σ^- have the same properties as M_σ : they are symmetrical and bloc-diagonal. One can remark that the matrix M_σ^+ is symmetrical positive defined.

Remark 2 (PML and fictitious domains) *Our new model is compatible with the PML and fictitious domains.*

4.4 Parameter estimation

We have to find the coefficient values of C and D using experimental data which are velocities and attenuation data for several angles for P-waves and S-waves (see [4]). We estimate the tensor in the same way as it is done in the elastodynamic case (estimation of C only).

For a given propagation direction, we build a modified Christoffel tensor $\bar{\Gamma}$ with the complex tensor $\bar{C} = i\omega(i\omega + D)^{-1}C$. One can show that the matrix $\bar{\Gamma}$ has two complex eigenvalues $\rho\left(\frac{v_P}{1 - i\frac{\gamma_P v_P}{\omega}}\right)^2$ and $\rho\left(\frac{v_S}{1 - i\frac{\gamma_S v_S}{\omega}}\right)^2$ where v_P and v_S are the wave velocties,γ_P and γ_S are the space attenuation for the P-waves and S-waves.

The parameter estimation is done with the weighted least squares method. The possibility of using different weights allow us to take into account measurement errors. The optimization takes into account the constraints that C and $C^{-1}D$ are symmetrical.

Remark 3 (A work at a given frequency !!) *In the parameter estimation, we assume that we are at a given frequency. Consequently, the tensors are only valid for that frequency (or possibly in a not too large bandwidth) and we have to do the simulations at this frequency.*

4.5 Numerical results

4.5.1 Numerical validation

According to the theory (see [1]), the P-wave attenuation is a raising curve towards the propagation angle,and the S-wave has a maximum in 45° (see figure 14). Unfortunately, the experimental P-wave attenuation data does not give a raising curve and is not in accord with the theory. Consequently, we choose low weights for the P-wave attenuation data. The profil of the S-wave attenuation is globally in accord with the theory, except for the 45° value. A low weight is taken for this value because it seems to be a measurement error.

The numerical validation consists in comparing the velocities (see figure 13) and attenuation (see 14) given by the experimental data with the theoritical values from the continuous equations with the tensors C and D and the numerical meausure from the simulated signal. To obtain these last data, we measure the signal at different points on the domain. The attenuation is obtained by comparing the maximum of each signal and in taking into account the distance between the measurement points. We can easily compute the wave velocity by comparing the times for which the signal maximum is obtained.

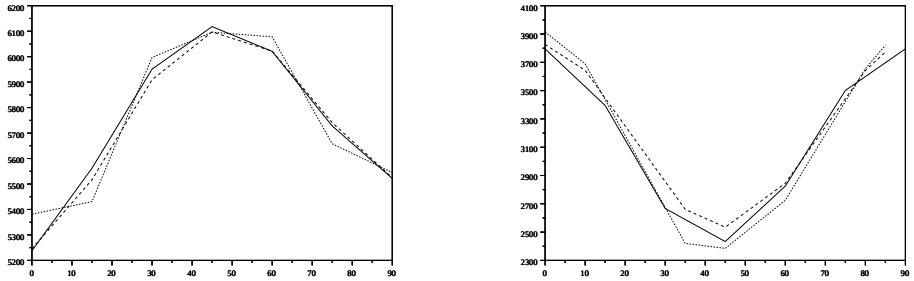

Figure 13: Results of the simulation (full line) to compare to the results of the and experiment ones (dashed lines). For the velocity of the P-wave (on left) and T-waves (on right) in function of the orientation.

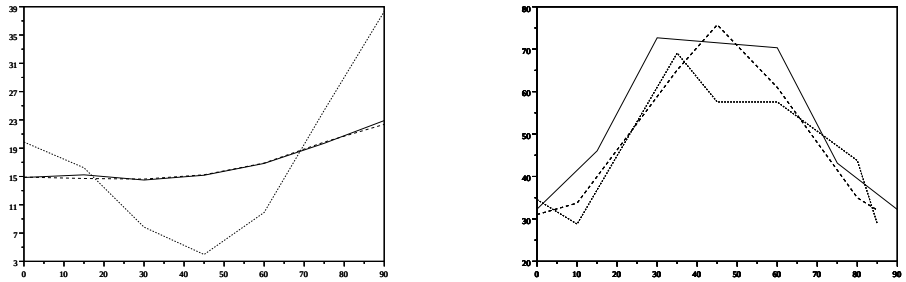

Figure 14: Results of the simulation (full line) to compare to the results of the and experiment ones (dashed lines). For the attenuation of the P-wave (on left) and T-waves (on right) in function of the orientation.

References

[1] S. Ahmed, R.B. Thompson. *Effect of preferred grain orientation and grain elongation on ultrasonic wave propagation in stainless steel.* Review of Progress in Quantitative Non Destructive Evaluation. 1992, Vol. 11, p. 1999-2006. (1992).

[2] J. Diaz *Prise en compte du bruit de structure dans la modélisation et la simulation d'expériences de contrôle non destructif.* Note interne EDF HI-23/06/005/A (à paraître). (2006).

[3] J. MOYSAN, A. APFEL, G. CORNELOUP, B. CHASSIGNOLE. Modelling the Grain Orientation of Austenitic Stainless Steel Multipass Welds to Improve Ultrasonic Assesment of Structural Integrity, International Journal of Pressure Vessels and Piping, Vol 80 n°2, 2003, pp 77 - 85

[4] M.-A. Ploix, R. El Guerjouma, J. Moysan, G. Corneloup, B. Chassignole. *Acoustical characterisation of austenitic stainless steel welds for experimental and modelling NDT.* Journal of advanced sciences, 2005 vol.17, $n°1\&2$, p.76-81 (2005).

[5] C. Tsogka. *Modélisation mathématique et numérique de la propagation des ondes élastiques tridimensionnelles dans des milieux fissurés.* Thèse, Univ. Paris IX. (1999).